Journal of Photochemistry and Photobiology A: Chemistry 293 (2014) 12–25

Contents lists available at ScienceDirect

Journal of Photochemistry and Photobiology A: Chemistry

journal homepage: www.elsevier.com/locate/jphotochem

Synthesis and chemiluminescent properties of 6,8-diaryl-2-methylimidazo[1,2-*a*]pyrazin-3(7*H*)-ones: Systematic investigation of substituent effect at *para*-position of phenyl group at 8-position

Ryota Saito[a,b,*], Takashi Hirano[c], Shojiro Maki[c], Haruki Niwa[c]

[a] *Department of Chemistry, Toho University, 2-2-1 Miyama, Funabashi, Chiba 274-8510, Japan*
[b] *Research Center for Materials with Integrated Properties, Toho University, Chiba, Japan*
[c] *Department of Engineering Science, Graduate School of Informatics and Engineering, The University of Electro-Communications, 1-5-1 Chofugaoka, Chofu, Tokyo 182-8585, Japan*

ARTICLE INFO

Article history:
Received 7 June 2014
Received in revised form 14 July 2014
Accepted 18 July 2014
Available online 28 July 2014

Keywords:
Imidazo[1,2-*a*]pyrazin-3(7*H*)-one
Chemiluminescence
Substituent effect

ABSTRACT

6,8-Diphenylimidazopyrazinone derivatives having a substituent R (R = CF_3, H, and OMe) at *para* position of the 8-phenyl group were synthesized and their chemiluminescent properties were investigated. The chemiluminescence maxima (CL_{max}) of these compounds were observed to be in the range of 513–553 nm with a bathochromic shift that increased with the electron-withdrawing character of R, contrary to the previously observed substituent effect at the 6-postion. The chemiluminescence efficiencies (ϕ_{CL}) of these imidazopyrazinones were improved by the introduction of a *p*-substituted phenyl group at the 8-position. The quantitative investigation of the three quantum efficiencies (ϕ_R, ϕ_S, and ϕ_{FL}) whose product gives us ϕ_{CL} revealed that the ϕ_{CL} gains made were largely because of the increase in the values of the fluorescence quantum yields of the corresponding light emitters (ϕ_{FL}). The yields of the singlet-excited emitters (ϕ_S) during the chemiluminescent reaction were found to be very small (0.015–0.019), suggesting that one cannot construct an efficient imidazopyrazinone–chemiluminescence system that is comparable to the aequorin bioluminescence system only by using the electronic effects of substituents.

1. Introduction

3,7-Dihydroimidazo[1,2-*a*]pyrazine-3-ones are widely distributed as luminescent substrates in the bioluminescent systems of various luminous marine organisms such as a photoprotein, aequorin, isolated from the jellyfish *Aequorea victoria* [1]. During the bioluminescent reaction of aequorin, coelenterazine (**1**) that is located at the reaction center of aequorin is oxidized to form coelenteramide (**2**) in its singlet-excited state. This reaction has high efficiency, one of the characteristics of aequorin bioluminescence [2,3]. Coelenterazine also undergoes a chemiluminescent reaction in aprotic solvents such as dimethyl sulfoxide (DMSO) under air in the absence of catalyzing proteins [4]. Various studies have focused on the mechanisms of bio- and chemiluminescence, and it has been predicted that the bio- and chemiluminescent reactions of coelenterazine follow the same molecular mechanism. The widely accepted mechanism for luminescent oxidation is shown in Scheme 1 [5]. The most important process in this mechanism is the decomposition of the dioxetanone intermediate **I** that results in the chemical generation of the singlet-excited state of the light emitter **II** [6–8]. Although the molecular mechanisms of bio- and chemiluminescence are identical, there is a considerable difference in their luminescent efficiencies. The chemiluminescence efficiency of coelenterazine (0.002 in DMSO) [4] is much lower than the bioluminescence efficiency of aequorin (0.2) [2]. Many studies have attempted to elucidate this difference in the mechanisms of bio- and chemiluminescence.

* Corresponding author at: Toho University, Department of Chemistry, 2-2-1 Miyama, Funabashi, Chiba 2748510 Japan. Tel.: +81474721926; fax: +81474721926.
E-mail address: saito@chem.sci.toho-u.ac.jp (R. Saito).

http://dx.doi.org/10.1016/j.jphotochem.2014.07.016
1010-6030/

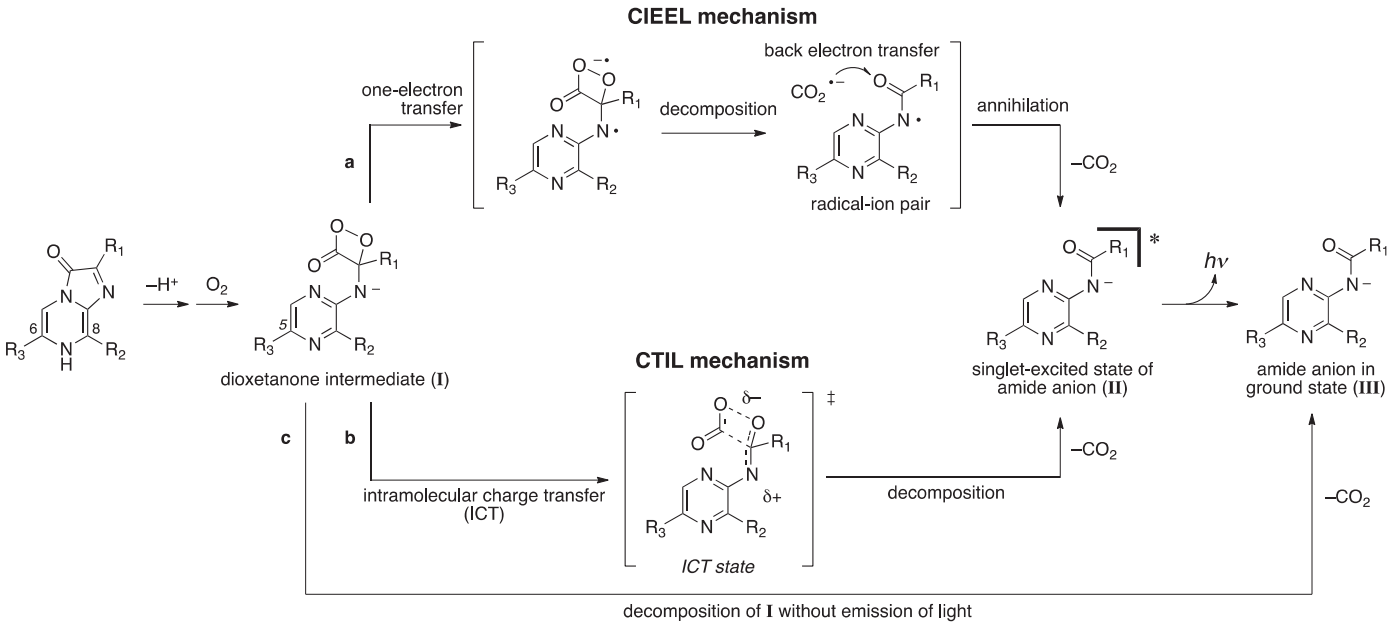

Scheme 1. Plausible reaction mechanism during the chemi- and bio-luminescent reactions of imidazopyrazinones.

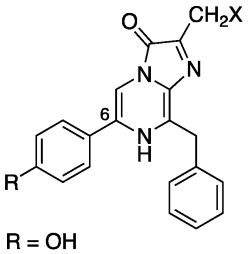

1: R = OH
X = 4-OH-C_6H_4
3: R = CF_3, F, H, OMe, NMe_2
X = H

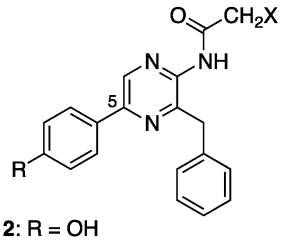

2: R = OH
X = 4-OH-C_6H_4
4: R = CF_3, F, H, OMe, NMe_2
X = H

The efficient generation of the singlet-excited emitter can be attributed to a chemically initiated electron exchange luminescence (CIEEL) mechanism [9] or a charge transfer-induced luminescence (CTIL) [8,10,11] mechanism. Scheme 1 illustrates the application of these mechanisms to the imidazopyrazinone bio- or chemi-luminescence sequence.

According to these hypotheses, the electron transfer from the amidopyrazine moiety to the dioxetanone ring promotes the decomposition of the dioxetanone intermediate, generating the singlet-excited amide anion with high efficiency [12]. In the case of the bioluminescent reaction of coelenterazine (**1**), the electron-donating hydroxyl group, which probably dissociates to form the more strongly electron-donating phenoxide in aequorin [13], is considered to be essential for the effective formation of the singlet-excited coelenteramide [14]. In order to understand the mechanism of bio- and chemi-luminescence of imidazopyrazinones and, in particular, to clarify whether the electron-donating substituent plays an important role in efficient generation of the singlet-excited emitter, we have been investigating systematically the substituent effects on the chemiluminescence of the coelenterazine analogues (**3**) [7,15] and on the fluorescence of the coelenteramide analogues (**4**) [16]. It was found that the efficiencies of the chemical generation of the singlet-excited light emitters (ϕ_S: 0.008–0.015) were quite small despite the large variation in the Hammett substituent constant of R from −0.83 (for NMe_2) to 0.54 (for CF_3). Although the substituent effect was apparently observed on the ϕ_S values, the variation in the ϕ_S values was so small that one cannot judge the relevance of the CIEEL or the CTIL mechanism using only these results. Therefore, these mechanisms are still controversial and the accumulation of related data is required.

We have also reported the chemiluminescence of some imidazopyrazinones that have a conjugated system at the 8-position of imidazopyrazinone nucleus in aqueous media [17,18]. These compounds mostly exhibited red-shifted chemiluminescence (λ_{max}: 500–530 nm) in basic buffer solutions, indicating that the chemiluminescent properties of imidazopyrazinones are strongly susceptible to the electronic substituent effect at the 8-position. However, since then, no attempt has been made to investigate systematically the substituent effect on chemiluminescent properties including chemiluminescence quantum yields.

As part of our ongoing efforts to understand and regulate the chemiluminescence of imidazopyrazinones using substituent effects, we synthesized imidazopyrazinones having *para*-substituted phenyl groups on their 8-position, **5a**–**c**, in which the electronic property of the substituents was systematically varied from electron-withdrawing (e.g., trifluoromethyl) to electron-donating (e.g., methoxy group). Herein, we report the effect of substituent variation on the chemiluminescent properties of **5a**–**c**. In addition, the syntheses and fluorescence of acetamidopyrazines, **6a**–**c**, which are the corresponding products obtained as a result of the oxidative chemiluminescence reactions of **5a**–**c**, have also been reported for a detailed understanding of the substituent effect on chemiluminescence.

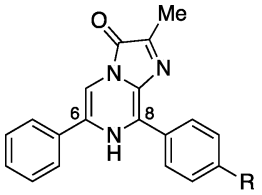

5a: R = CF_3
5b: R = H
5c: R = OMe

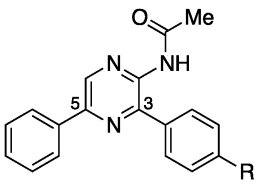

6a: R = CF_3
6b: R = H
6c: R = OMe

2. Experimental

2.1. General

All melting points were measured on a YAMATO Model MP-21 or a LABORATORY DEVICES Mel-Temp II apparatuses in open capillaries and are uncorrected. ^{1}H-NMR spectra were recorded on a JNM-GX270 spectrophotometer (JEOL Ltd., Japan) or a JNM-LA400 spectrophotometer (JEOL Ltd., Japan). Chemical shifts (δ) are reported in ppm using tetramethylsilane or an undeuterated solvent as internal standards in the deuterated solvent used. Coupling constants (J) are given in Hz. Chemical shift multiplicities are reported as s = singlet, d = doublet, t = triplet, and m = multiplet. Infrared (IR) spectra were obtained using the spectrophotometers IR-810 or FT/IR-470plus (JASCO Co., Ltd., Japan). High and low resolution electron impact ionization (EI) mass spectra were measured on a HITACHI Model M-80B mass spectrometer with a HITACHI M-0101 data system. The ionization energy and the accelerating voltage were 70 eV and 3 kV, respectively. Combustion analyses were performed on a PERKIN ELMER Series II CHNS/O Analyzer 2400. All conventional chemicals used in the present study are commercially available, and were used as received.

2.2. Computational details

Semi-empirical calculations for ground and singlet-excited states geometries were carried out with the PM7 [19] method of MOPAC 2012 [20]. Solvent's dielectric constant was taken into account for these calculations by applying the conductor-like screening (COSMO) model [21]. Density functional theory (DFT) calculations [22], which include time-dependent DFT (TDDFT) method [23], were performed with the GAMESS program (version 11) [24,25] using Becke's three-parameter function combined with Lee, Yang and Parr's correlation function (B3LYP) [26]. The DFT calculations for geometry optimizations were performed with the 6-31G(d) (for neutral compounds) or the 6-31+G(d) [27] (for anionic compounds) basis set, and the TDDFT calculations were carried out with the 6-31+G(d) basis set. Analysis of the MOPAC and GAMESS log-files as well as molecular graphics were carried out using the Winmostar™ program [28] and Chem3D Pro (ver. 12.0). Semi-empirical quantum calculations of the UV/vis absorption spectra were achieved by the intermediate neglect of differential overlap/screened (INDO/S) approximation method [29] using the Winmostar™ with the following parameters: basis function = SDP, repulsion integral formula = "3" (Nishimoto-Mataga equation), charge = 0, nuclear repulsion formula = "2" (Za*Zb*γab), PKappa (Kappa value for p electron) = 0.585, DKappa (Kappa value for d electron) = 0.3, CI = 20, and number of excited states = 1. All calculations were conducted on a PC carrying an Intel Core™ i3 3220 processor (3.30 GHz) and 8-GB RAM.

2.3. Chemiluminescence spectra

Chemiluminescence spectra of the imidazopyrazinones **5a**–**c** were measured on a PMA-10 photonic multichannel analyzer equipped with an image intensifier (Hamamatsu Photonics K. K.). Chemiluminescence measurement was achieved by mixing a stock solution (100 μl) of **5a**–**c** in methanol (1.0 mM) and DMSO (2.0 ml) within a 1-cm^2 quartz cuvette under aerobic condition at 25 °C. The reproducibility of each measurement was definitively verified.

2.4. Chemiluminescence quantum yields

The chemiluminescence quantum yields of **5a**–**c** at 25 °C were determined by comparing their luminescence intensities to that of luminol as a standard (ϕ_{CL} = 0.028) [30]. The luminescence intensities were recorded on a TD-4000 lumiphotometer (Laboscience Co., Tokyo, Japan). The condition for this experiment is as follows: a 15-μl methanolic solution of **5a**–**c** (4.0 μM) was placed in the lumiphotometer, and the chemiluminescence reaction was initiated by the injection of 300 μl of dehydrated DMSO.

2.5. Uv–vis absorption and fluorescence spectrometry

Spectral grade solvents were used for the measurement of UV–vis absorption and fluorescence spectra. UV–vis spectra were recorded on a Model 320 (Hitachi Co., Ltd., Japan) or a V-550 spectrophotometer (JASCO Co., Ltd., Japan). Fluorescence spectra were measured with a Model F-4010 (Hitachi Co., Ltd., Japan) or a Model F-777 fluorescence spectrophotometer (JASCO Co., Ltd., Japan) and corrected according to the manufacturer's instructions (excitation bandpass: 5 nm; emission bandpass: 5 nm; response: 2.0 s; scan speed: 60 nm min^{-1}). A solution of compound **4** or **6** for fluorescence measurement was prepared by mixing a stock solution (100 μl) of **4** or **6** in DMSO (20 μM) and DMSO containing 0.5 vol% of 10%-methanolic tetrabutylammonium hydroxide (2.0 ml) within a 1-cm^2 quartz cuvette at 25 °C. The reproducibility of each measurement was definitively verified.

2.6. Fluorescence quantum yields [7,16]

The fluorescence quantum yields at 25 °C were measured relative to quinine bisulfate in 0.1 M sulfuric acid and calculated on the basis of the following equation.

$$\phi_f^{sam} = \phi_f^{ref} \frac{n_{ref}^2}{n_{sam}^2} \frac{OD_{ref}}{OD_{sam}} \frac{\int I_f^{sam}\left(\lambda_f^{sam}\right) d\lambda_f^{sam}}{\int I_f^{ref}\left(\lambda_f^{ref}\right) d\lambda_f^{ref}}$$

where n_{ref} and n_{sam} are the refractive indices of the solvents, OD_{ref} and OD_{sam} ($\leq$0.02) are the optical densities, ϕ_f^{ref} (=0.52) and ϕ_f^{sam} are the quantum yields, and the integrals denote the (computed) area of the corrected fluorescence spectra, each parameter for the standard (ref) and sample (sam) solutions, respectively. The reproducibility of each measurement was definitively verified.

2.7. Determination of ϕ_R values

The ϕ_R values were determined by comparing the HPLC chromatogram of the luminescence-spent product with that of the corresponding synthesized acetamidopyrazine **6a**–**e**. The HPLC analyses were performed on an Inertsil ODS column (4.6 × 250 mm; GL Sciences, Inc., Japan) with an acetonitrile/water solvent system as a mobile phase.

2.8. Synthetic procedures

2.8.1. Representative procedure for the Suzuki coupling reactions. A typical example: Synthesis of 2-amino-5-bromo-3-(4-trifluoromethylphenyl)pyrazine (**9a**) and 2-amino-3,5-bis(4-trifluoromethylphenyl)pyrazine (**10a**)

To a dioxane solution (6.0 ml) of 2-amino-3,5-dibromopyrazine **7** (304 mg, 1.20 mmol) was successively added tetrakis (triphenylphosphine)palladium (112 mg, 9.6 × 10^{-5} mol, 8 mol%), 4-trifluoromethylphenylboronic acid **8a** (230 mg, 1.21 mmol), and 1 ml of 2-mol dm^{-3} sodium carbonate under argon atmosphere. The mixture was then refluxed for 4 h under argon atmosphere. After cooling to room temperature, water (10 ml) was added, and organic materials were extracted using chloroform (15 ml × 3). The combined organic layer was then dried over sodium sulfate. The removal of the solvent afforded brown solid, which was purified by

preparative thin-layered chromatography on Merck silica gel (particle size, 5–40 μm; 200 × 200 × 1.75 mm, 5 plates) with a mixed solvent system (ethylacetate:hexane = 8:3) as a mobile phase to give **9a** (293 mg, 77%) in the form of a pale yellow solid and **10a** (17 mg, 4%) in the form of a pale yellow solid. **9a**: *mp*152–154 °C (ethanol–hexane); δ_H (400 MHz, $CDCl_3$) 4.78 (br. s, 2*H*), 7.77 (d, *J* = 8.3, 2*H*), 7.88 (d, *J* = 8.3, 2*H*), 8.13 (s, 1*H*); ν_{max} (KBr)/cm^{-1} 3415, 3311, 3185, 1642, 1616, 1449, 1406, 1320, 852; *m/z* (positive-EI) (relative intensity) 319 (93), 317 (M^+, 100), 211 (61), 184 (47). Anal. Calcd for $C_{11}H_7BrF_3N_3$: C, 41.53; H, 2.22; N, 13.21. Found: C, 41.94; H, 2.06; N, 12.89. **10a**: *mp* 194–196 °C (ethanol–hexane); δ_H (400 MHz, $CDCl_3$) 4.94 (br. s, 2*H*), 7.70 (d, *J* = 8.0, 2*H*), 7.80 (d, *J* = 8.0, 2*H*), 7.96 (d, *J* = 8.0, 2*H*), 8.07 (d, *J* = 8.0, 2*H*), 8.55 (s, 1*H*); ν_{max} (KBr)/cm^{-1} 3482, 3288, 3152, 1630 (sh), 1618, 1536, 1464, 1425, 1408, 1329, 852; *m/z* (positive-EI) (relative intensity) 383 (100, M^+), 382 (41), 356 (15), 314 (10). Anal. Calcd for $C_{18}H_{11}F_6N_3$: C, 56.40; H, 2.89; N, 10.96. Found: C, 56.54; H, 2.72; N, 10.86.

2.8.2. 2-Amino-5-bromo-3-(4-methoxyphenyl)pyrazine (**9c**)

Prepared from **7** (304 mg, 1.20 mmol) with tetrakis(triphenylphosphine)palladium (112 mg, 9.6×10^{-5} mol, 8 mol%), 4-methoxyphenylboronic acid **8c** (182 mg,1.20 mmol), and 1.5 ml of 2-mol dm^{-3} sodium carbonate using a method similar to that for preparing **9a**: yield, 171 mg (51%); *mp* 143–145 °C (ethanol–hexane); δ_H (400 MHz, $CDCl_3$) 3.87 (s, 3*H*), 4.76 (br. s, 2*H*), 7.01 (d, *J* = 9.0, 2*H*), 7.69 (d, *J* = 9.0, 2*H*), 8.03 (s, 1*H*); ν_{max} (KBr)/cm^{-1} 3470, 3292, 3146, 2827, 1631, 1609, 1508, 1440, 1391, 1251, 839. Anal. Calcd for $C_{11}H_{10}BrN_3O$: C, 47.16; H, 3.60; N, 15.00. Found: C, 47.28; H, 3.46; N, 14.85.

2.8.3. 2-Amino-3,5-bis(4-methoxyphenyl)pyrazine (**10c**)

This compound was obtained as a by-product in the synthesis of **5c**: yield, 44 mg (12%). Identification of the product was achieved by comparing its spectral features with that of previously reported data [31].

2.8.4. 2-Amino-5-phenylpyrazine (**13**)

Prepared from **12** (122 mg, 7.01×10^{-4} mol) with tetrakis (triphenylphosphine)palladium (33.5 mg, 2.90×10^{-5} mol), phenylboronic acid **8b** (116 mg, 9.53×10^{-4} mol), and 1.0 ml of 2-mol dm^{-3} sodium carbonate using a method similar to that for preparing **9a,** except refluxing for 12 h. The product was isolate by column chromatography on silica gel (particle size, 63–200 μm; 30 g), eluting with a mixed solvent system (ethylacetate:chloroform = 1:1), followed by recrystallization from ethanol–hexane to give **13** as tan needles: yield, 89.2 mg (74%); *mp*: 146–147 °C; δ_H (400 MHz, $CDCl_3$) 4.61 (br. s, 2*H*), 7.35–7.49 (m, 3*H*), 7.87–7.90 (m, 2*H*), 8.80 (d, *J* = 1.4, 1*H*), 8.46 (d, *J* = 1.4, 1*H*); ν_{max} (KBr)/cm^{-1} 3340, 3174, 3020, 1653, 1588, 1536, 1480, 1389, 751, 694 (γCH). Anal. Calcd for $C_{10}H_9N_3$: C, 70.16; H, 5.30; N, 24.54. Found: C, 70.32; H, 5.19; N, 24.63.

2.8.5. 2-Amino-3-bromo-5-phenylpyrazine (**14**)

To a solution of aminopyrazine **13** (902 mg, 5.27 mmol) in chloroform (40 ml) was added tetrabutylammonium tribromide (3.11 g, 6.44 mmol) and pyridine (7.0 ml) under argon atmosphere, and the mixture was then stirred for 3 h with heating on an oil bath (55–58 °C) under argon. After cooling to room temperature water was added to the reaction mixture, and then the mixture was stirred for another 20 min at room temperature. Organic materials were then extracted with chloroform (50 ml × 3), and the combined organic layer was dried over sodium carbonate. The removal of the solvent afforded black mass, which was purified by column chromatography on silica gel (particle size, 63–200 μm; 530 g), eluting with a mixed solvent system (ethylacetate:chloroform = 1:1) to give a yellowish brown solid of **14**. Yield: 1.16 g (88%); *mp* 133 °C (decomop); δ_H (270 MHz, $CDCl_3$) 5.06 (br. s, 2*H*), 7.34–7.48 (m, 3*H*), 7.84–7.89 (m, 2*H*), 8.41 (s, 1*H*); *m/z* (positive-EI) (relative intensity) 251 (91, $[M+2]^+$), 249 (100, M^+), 170 (17), 143 (20), 116 (62).

2.8.6. 2-Amino-5-phenyl-3-(4-trifluoromethylphenyl)pyrazine (**11a**)

Method A (from **9a**): In this method **11a** was prepared from **7** (137 mg, 4.30×10^{-4} mol) with tetrakis(triphenylphosphine)palladium (25 mg, 2.1×10^{-5} mol), 4-trifluoromethylphenylboronic acid **8a** (57.3 mg, 4.70×10^{-4} mol), and 0.5 ml of 2-mol dm^{-3} sodium carbonate using a method similar to that for preparing **9a**. Yield: 111 mg (82%). **Method B** (from **14**): **11a** was prepared from **14** (251 mg, 1.00 mmol) with tetrakis(triphenylphosphine)palladium (43 mg, 3.7×10^{-5} mol), 4-trifluoromethylphenylboronic acid **8a** (285 mg, 1.5 mmol), and 0.9 ml of 2-mol dm^{-3} sodium carbonate i using a method similar to that for preparing **9a**, except refluxing for 9 h. The product was isolated by column chromatography on silica gel (particle size, 63–200 μm; 100 g) with a mixed solvent system (ethylacetate:chloroform = 4:1) as eluents. Yield: 301 mg (95%). Compound **11a** was obtained as tan needles (from ethanol); *mp* 190–190 °C; δ_H (270 MHz, $CDCl_3$) 4.78 (br. s, 2*H*), 7.35–7.49 (m, 3*H*), 7.79 (d, *J* = 8.6, 2*H*), 7.95–8.00 (m, 4*H*), 8.51 (s, 1*H*); ν_{max} (KBr)/cm^{-1} 3405, 3305, 3172, 1641, 1614, 1530, 1465, 1406, 1322, 849, 762, 695; *m/z* (positive-EI) (relative intensity) 315 (100, M^+), 288 (23), 102 (68). HRMS (positive-EI) Calcd for $C_{17}H_{12}F_3N_3$: 315.0983. Found: 315.1038.

2.8.7. 2-Amino-3,5-diphenylpyrazine (**11b**)

Prepared from **7** (401 mg, 1.59 mmol) with tetrakis (triphenylphosphine)palladium (72 mg, 6.2×10^{-5} mol), phenylboronic acid **8b** (491 mg, 4.03 mmol), and 8.0 ml of 2-mol dm^{-3} sodium carbonate using a method similar to that for preparing **9a**, except refluxing for 5 h in 1,2-dimethoxyehane. The product was isolate by column chromatography on silica gel (particle size, 63–200 μm; 70 g), eluted with a mixed solvent system (first ethylacetate:chloroform:hexane = 1:1:1, and then ethylacetate:chloroform = 1:1) to give **11b** as pale yellow solids. Yield: 360 mg (91%); *mp* 134–135 °C; δ_H (270 MHz, $CDCl_3$) 4.84 (br. s, 2*H*), 7.32–7.56 (m, 6*H*), 7.80–7.84 (m, 2*H*), 7.95–7.99 (m, 2*H*), 8.45 (s, 1*H*); ν_{max} (KBr)/cm^{-1} 3461, 3282, 3144, 1625, 1536, 1459, 1436, 746, 688; *m/z* (positive-EI) (relative intensity) 247 (100, M^+), 220 (17), 116 (12), 102 (22), 89 (10). HRMS (positive-EI) Calcd for $C_{16}H_{13}N_3$: 247.1108. Found: 247.1085.

2.8.8. 2-Amino-5-phenyl-3-(4-methoxyphenyl)pyrazine (**11c**)

Method A (from **9c**): In this method **11c** was prepared from **9c** (114 mg, 4.07×10^{-4} mol) with tetrakis(triphenylphosphine)palladium (25 mg, 2.1×10^{-5} mol), 4-methoxyphenylboronic acid **8c** (57 mg, 4.7×10^{-4} mol), and 0.5 ml of 2-mol dm^{-3} sodium carbonate in using a method similar to that for preparing **9a**. Yield: 109 mg (96%). **Method B** (from **14**): In this method **11c** was prepared from **14** (50 mg, 0.2 mmol) with tetrakis(triphenylphosphine)palladium (21 mg, 1.8×10^{-5} mol), 4-methyoxhyphenylboronic acid **8c** (40 mg, 0.26 mmol), and 0.3 ml of 2-mol dm^{-3} sodium carbonate using a method similar to that for preparing **9a**, except refluxing for 13 h in 1,2-dimethoxyethane. Yield: 52 mg (94%). Compound **11c** was obtained as tan needles (from ethanol); *mp* 138–139 °C; δ_H (270 MHz, $CDCl_3$) 4.78 (br. s, 2*H*), 7.05 (d, *J* = 8.9, 2*H*), 7.32–7.47 (m, 3*H*), 7.79 (d, *J* = 8.9, 2*H*), 7.94–7.99 (m, 4*H*), 8.42 (s, 1*H*); ν_{max} (KBr)/cm^{-1} 3449, 3305, 3170, 1636, 1608, 1533, 1510, 1461, 1245, 839, 766, 695; *m/z* (positive-EI) (relative intensity) 277 (100, M^+). HRMS (positive-EI) Calcd for $C_{17}H_{15}N_3O$: 277.1215. Found: 277.1188.

*2.8.9. 3,7-Dihydro-2-methyl-6-phenyl-8-(4-trifluoromethyl-phenyl)imidazo[1,2-a]pyrazin-3-one (**5a**)*

To a degassed ethanol solution (2.5 ml) of **11a** (81 mg, 0.26 mmol) was added pyruvic aldehyde (40 wt% solution in water, 175 mg, 0.97 mmol) and conc. HCl (100 μl). The mixture was heated at 80 °C in a sealed-vessel under argon atmosphere for 3.5 h. After cooling to room temperature, the solvent was removed under reduced pressure. Diethyl ether (1.0 ml) and concentrated hydrogen chloride (2 drops) were successively added to the residue and the mixture was cooled to −20 °C to form yellow precipitate, which was collected by suction filtration. After drying *in vacuo*, the hydrochloride salt of **5a** was obtained as pale yellow solids. Yield: 71 mg (68%); *mp* 153 °C (decomp); δ_H (400 MHz, CD_3OD) 2.55 (s, 3*H*), 7.49–7.59 (m, 3*H*), 8.00 (d, *J* = 8.1, 2*H*), 8.15–8.18 (m, 2*H*), 8.30 (d, *J* = 8.1, 2*H*), 8.79 (s, 1*H*); ν_{max} (KBr)/cm^{-1} 3403, 3067, 2931, 1658, 1572, 1532, 1493, 1323, 848, 770, 695. Anal. Calcd for $C_{20}H_{14}F_3N_3O{\cdot}HCl$: C, 61.98; H, 3.77; N, 10.84. Found: C, 62.09; H, 3.60; N, 10.79. The hydrochloride-free **5a** was readily obtained by passing through a silica-gel short column with 10:1 chloroform/methanol as eluents. HRMS (positive-EI) Calcd for $C_{20}H_{14}F_3N_3O$:369.1089. Found: 369.1011.

*2.8.10. 3,7-Dihydro-2-methyl-6,8-diphenylimidazo[1,2-a] pyrazin-3-one (**5b**)*

Prepared from **11b** (110 mg, 0.44 mmol) using a method similar to that for preparing **5a**. The Product, **5b** hydrochloride, was obtained as yellow needles (71 mg, 49%). *mp* 128 °C (decomp); δ_H (400 MHz, CD_3OD) 2.55 (s, 3*H*), 7.48–7.58 (m, 3*H*), 7.67–7.73 (m, 3*H*), 8.06–8.10 (m, 2*H*), 8.14–8.16 (m, 2*H*), 8.75 (s, 1*H*); ν_{max} (KBr)/cm^{-1} 3401, 3061, 2924, 1658, 1572, 1528, 1492, 773, 694. Anal. Calcd for $C_{19}H_{15}N_3O{\cdot}HCl{\cdot}0.75H_2O$: C, 64.96; H, 5.02; N, 11.96. Found: C, 65.24; H, 4.95; N, 11.44. HRMS (positive-EI) Calcd for $C_{19}H_{15}N_3O$: 301.215. Found: 301.1263.

*2.8.11. 3,7-Dihydro-8-(4-methoxyphenyl)-2-methyl-6-phenylimidazo[1,2-a]pyrazin-3-one (**5c**)*

Prepared from **11c** (90 mg, 0.32 mmol) using a method similar to that for preparing **5a**. The Product, **5c** hydrochloride, was obtained as yellow needles (63 mg, 54%). *mp* 129 °C (decomp); δ_H (400 MHz, CD_3OD) 2.55 (s, 3*H*), 7.23 (d, *J* = 8.8, 2*H*), 7.50–7.59 (m, 3*H*), 8.09–8.12 (m, 2*H*), 8.11 (d, *J* = 8.8, 2*H*), 8.64 (s, 1*H*); ν_{max} (KBr)/cm^{-1} 3406, 3071, 2935, 1660, 1607, 1534, 1493, 1026, 887, 766, 693. Anal. Calcd for $C_{20}H_{17}N_3O_2{\cdot}HCl{\cdot}2.1H_2O$: C, 59.22; H, 5.52; N, 10.36. Found: C, 58.95; H, 5.02; N, 10.34. HRMS (positive-EI) Calcd for $C_{20}H_{17}N_3O_2$: 331.1321. Found: 331.1364.

*2.8.12. 2-Acetamino-5-phenyl-3-(4-trifluoromethylphenyl) pyrazine (**6a**)*

A mixture of **11a** (50 mg, 0.16 mmol) and acetic anhydride (1.5 ml, 16 mmol) was stirred at 70 °C for 1d. After cooling to room temperature the resulting colorless precipitate was collected by suction filtration. The collected material was washed with water, and then purified by recrystallization from methanol to afford the product as colorless needles (14 mg, 24%). *mp* 218 °C; δ_H (270 MHz, DMSO-d_6) 1.95 (s, 3*H*), 7.48–7.60 (m, 3*H*), 7.85 (d, *J* = 8.2, 2*H*), 8.03 (d, *J* = 8.2, 2*H*), 8.19–8.22 (m, 2*H*), 9.13 (s, 1*H*), 10.63 (s, 1*H*); ν_{max} (KBr)/cm^{-1} 3430, 3220, 1670, 1328, 852; *m/z* (positive-EI) (relative intensity) 357 (39, M^+), 315 (100), 116 (58), 102 (56), 77 (37), 69 (78). HRMS (positive-EI) Calcd for $C_{19}H_{14}F_3N_3O$: 357.1089. Found: 357.1131.

*2.8.13. 2-Acetamino-3,5-diphenylpyrazine (**6b**)*

To a solution of **11b** (60 mg, 0.24 mmol) and anhydrous pyridine (0.70 ml, 8.6 mmol) in anhydrous dichloromethane (2.0 ml) was added dropwise acetyl chloride (80 μl, 1.1 mmol) at 0 °C in a period of 2 min, and the mixture was stirred for 30 min. Saturated aqueous sodium bicarbonate (2.0 ml) was added to the reaction mixture, and then organic materials were extracted with chloroform (10 ml × 3). The combined organic layer was dried over magnesium sulfate, and then the solvent was removed under reduced pressure to afford crude product, which was purified by recrystallization from methanol to give the pure product as colorless needles (41 mg, 58%). *mp* 183–184 °C; δ_H (270 MHz, DMSO-d_6) 1.93 (s, 3*H*), 7.41–7.59 (m, 6*H*), 7.83 (dd, *J* = 1.6, 7.9, 2*H*), 8.19 (dd, *J* = 1.6, 7.9, 2*H*), 9.05 (s, 1*H*), 10.40 (s, 1*H*); ν_{max} (KBr)/cm^{-1} 3430, 3250, 1670, 1540, 1504, 1492, 1419, 749, 693; *m/z* (positive-EI) (relative intensity) 289 (14, M^+), 247 (61), 116 (37), 102 (39), 89 (47), 43 (100). HRMS (positive-EI) Calcd for $C_{18}H_{15}N_3O$: 289.1215. Found: 289.1219.

*2.8.14. 2-Acetamino-5-phenyl-3-(4-methoxyphenyl)pyrazine (**6c**)*

Prepared from **11c** (101 mg, 0.36 mmol) using a method similar to that for preparing **6b**. Yield: 62 mg (53%), colorless needles (from methanol); *mp* 193 °C; δ_H (270 MHz, DMSO-d_6) 1.96 (s, 3*H*), 3.83 (s, 3*H*), 7.04 (d, *J* = 8.9, 2*H*), 7.47–7.59 (m, 3*H*), 7.82 (d, *J* = 8.9, 2*H*), 8.18 (dd, *J* = 1.6, 7.9, 2*H*), 8.99 (s, 1*H*), 10.34 (s, 1*H*); ν_{max} (KBr)/cm^{-1} 3450, 3240, 1671, 1510, 1372, 1254, 1178; *m/z* (positive-EI) (relative intensity) 319 (45, M^+), 277 (61), 116 (63), 102 (64), 89 (42), 43 (83). HRMS (positive-EI) Calcd for $C_{19}H_{17}N_3O_2$: 319.1312. Found: 319.1280.

*2.8.15. 3,7-Dihydro-2-methyl-8-(2,6-dimethylphenyl)-6-phenylimidazo[1,2-a]pyrazin-3-one (**16**)*

To a mixture of **7** (211 mg, 0.84 mmol), 2,6-dimethylphenylboronic acid (126 mg, 0.84 mmol) and triphenylphosphine (36 mg, 0.14 mmol) in dioxane (3.0 ml) were successively added bis(triphenylphosphine)palladium(II) dichloride (36 mg, 50.9 μmol) and aqueous sodium bicarbonate (2 M, 1.0 ml). The mixture was then refluxed for 16 h under argon atmosphere. After cooling to room temperature, water (40 ml) was added to the reaction mixture and organic materials were extracted with chloroform (50 ml × 3). The combined organic layer was dried over magnesium sulfate, and the solvent was evaporated to give brownish amorphous, which was roughly purified by column chromatography on silica gel to give orange glassy solid that contained 2-amino-5-bromo-3-(2,6-dimethylphenyl)pyrazine. This material was directly reacted with phenylboronic acid (92 mg, 0.75 mmol) without further purification using a method similar to that for preparing **11a**, yielding **15** (95 mg, 41% from **7**) as pale yellow solid; δ_H (400 MHz, $CDCl_3$) 2.13 (s, 6*H*), 4.46 (br, s, 2*H*), 7.17 (d, *J* = 7.3, 2*H*), 7.26 (t, *J* = 7.3, 1*H*), 7.33–7.37 (m, 1*H*), 7.42–7.45 (m, 2*H*), 7.91–7.93 (m, 2*H*), 8.48 (s, 1*H*). Then, **15** was reacted with pyruvic aldehyde using a method similar to that for preparing **5a** hydrochloride. The obtained **16** hydrochloride was purified by column chromatography on silica gel with chloroform/methanol (10/1) as eluents to afford hydrochloride-free **16**. Yield: 69 mg (70% from **15**), orange solid; δ_H (400 MHz, $CDCl_3$) 2.29 (s, 6*H*), 2.45 (s, 3*H*), 7.15 (s, 1*H*), 7.18 (d, *J* = 7.6, 2*H*), 7.31 (t, *J* = 7.8, 1*H*), 7.44–7.54 (m, 6*H*); ν_{max} (KBr)/cm^{-1} 3430, 3034, 2918, 1631, 1558, 1505, 1469, 768, 694, 674. Anal. Calcd for $C_{20}H_{17}N_3O_2{\cdot}HCl{\cdot}2.1H_2O$: C, 59.22; H, 5.52; N, 10.36. Found: C, 58.95; H, 5.02; N, 10.34.

3. Results and discussion

3.1. Syntheses and electronic properties of imidazopyrazinones **5a–c**

The preparation of the imidazopyrazinones was achieved in accordance with Scheme 2. The starting material, 2-amino-3,

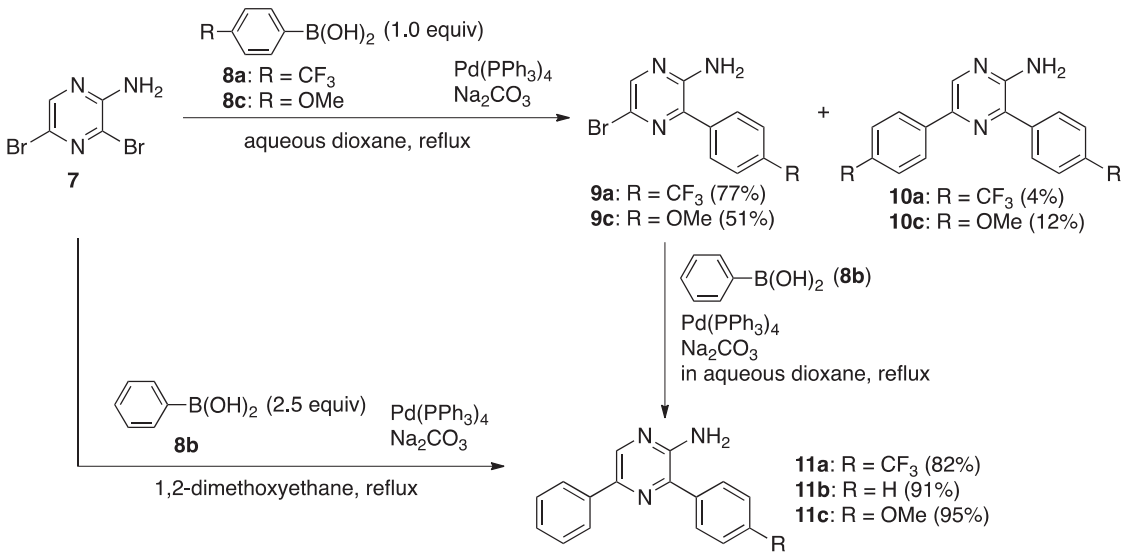

Scheme 2. Synthesis pathways for 2-amino-3,5-diarylpyrazines **11a–c**.

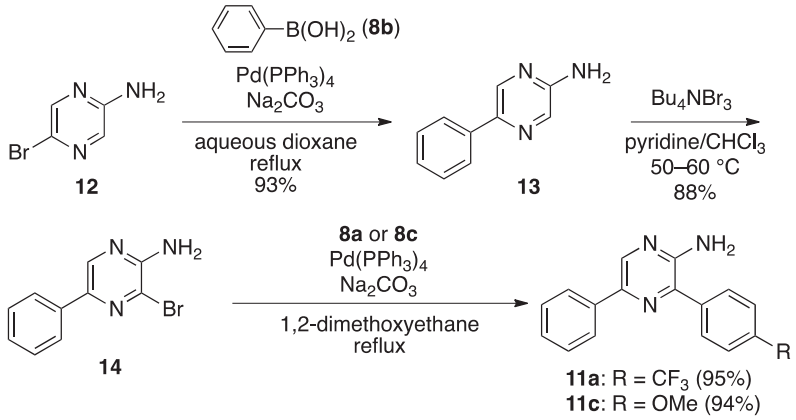

Scheme 3. Alternative methods for preparing 2-amino-3,5-diarylpyrazines **11a** and **11c**.

5-dibromopyrazine (**7**), was prepared by the bromination of commercially available 2-aminopyrazine with tetrabutylammonium tribromide, a useful substituent for bromine [32], according to the method described in literature [33]. Next, the monoarylated aminopyrazines **9a** and **9c** were obtained in good yield by a regioselective palladium-catalyzed cross-coupling reaction of dibromopyrazine **7** with an equimolar of arylboronates **8a** and **8c**, respectively. A small amount of the corresponding 3,5-diarylated products (**10a**) [18] was also obtained. The C-3 selectivity was also observed in a Sonogashira coupling reaction [34] using the

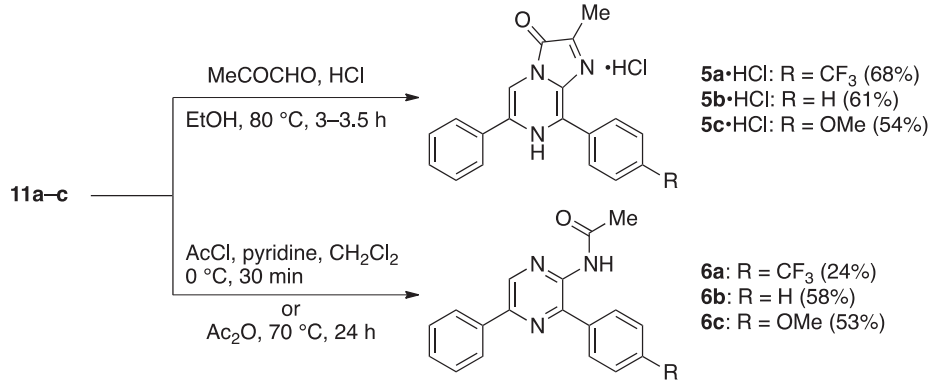

Scheme 4. Synthesis of imidazopyrazinones **5a–c** and amidopyrazines **6a–c**.

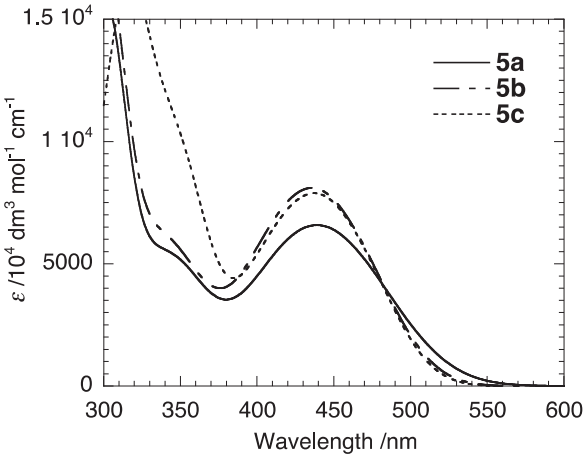

Fig. 1. Absorption spectra of the imidazopyrazinones **5a–c** (100 μM) in Britton–Robinson buffer (pH 7.0).

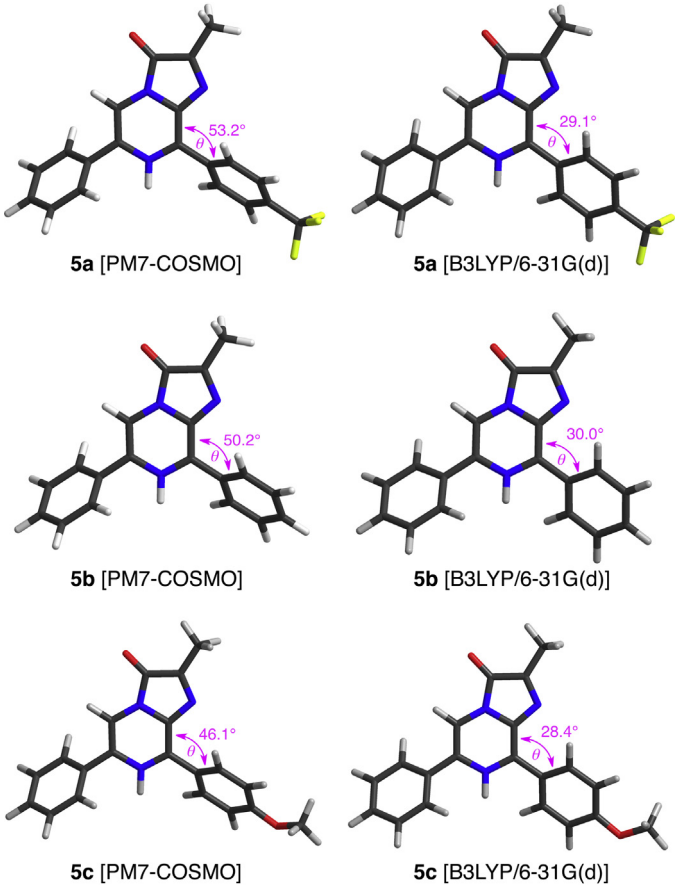

Fig. 2. Optimized geometries of **5a–c** calculated by the PM7-COSMO and the B3LYP/6-31G(d) methods.

same substrate. This regioselectivity may be caused by the vicinal contribution of the 2-amino group during the catalytic cycle. The resulting bromopyrazines **9a** and **9c** were then further reacted with phenylboronic acid **8b** under Suzuki-coupling conditions to afford the diarylaminopyrazines **11a** and **11c**, respectively. Thus, two different aryl substituents were introduced at 3- and 5-positions of 2-aminopyrazine by successive Suzuki coupling reactions. Diarylaminopyrazines **11a** and **11c** were also obtained from 2-amino-5-bromopyrazine **12** in three steps, as shown in Scheme 3. The spectroscopic features of the diarylaminopyrazines obtained by both the synthetic routes were identical, confirming the regioselective introduction of the different aryl groups. 2-Amino-3,5-diphenylpyrazine **11b** was directly synthesized by the Suzuki cross-coupling reaction of 2-amino-3,5-dibromopyrazine with two equivalents **8b** in good yield. Thus, the present study has provided additional examples of compounds obtained as a result of the introduction of different conjugate systems at the 3- and 5-positions of 2-aminopyrazine. The obtained 3,5-diarylaminopyrazines **11a–c** were then condensed with pyruvic aldehyde under acid-catalyzed conditions [7,34] to afford the intended imidazopyrazinones **5a–c** as hydrochloride salts in moderate yields (68% for **5a**, 49% for **5b**, and 53% for **5c**) (Scheme 4). 2-Acetamidopyrazines **6a–c**, the corresponding products of the oxidative chemiluminescent reactions of **5a–c**, were prepared by the acetylation of the 3,5-diarylaminopyrazine **11a–c** (Scheme 4) [16]. The structure of the products was verified using ^{1}H-NMR, IR, and high-resolution mass spectrometries, coupled with combustion analysis.

In order to understand the electronic effects of the phenyl group at the 8-position and the substituent R on the central imidazopyrazinone conjugate system, the electronic absorption spectra of the synthesized imidazopyrazinones **5a–c** were measured, and the results are shown in Fig. 1. Each compound exhibits the lowest transition at approximately 435 nm, which is almost equal to that of 3,7-dihydro-2-methyl-6-phenylimidazo[1,2-*a*]pyrazin-3-one, the *Cypridina* luciferin analogue (CLA) [35], having no substituent at the 8-position. In addition, the lowest transition energy is found to be independent of the electronic effect of the substituent even in a polar medium such as water. These results imply that the phenyl ring at the 8-position is twisted in such a manner that there is no interaction between the π-electrons of the central imidazopyrazinone and those of the phenyl group at the 8-position. The X-ray crystallographic analysis of **5a–c** would provide the evidence for this, but it has not been completed because single crystals of these compounds suitable for the analysis have been hardly obtained. Therefore, the optimized geometry of **5a–c** was estimated using both semi-empirical and density functional theory (DFT) [22,24] calculations. For semi-empirical approach, PM7 method [19] with the conductor-like screening model (COSMO) [21] was adopted, and DFT calculations were performed at the B3LYP/6-31G(d) level [26]. The results are shown in Fig. 2. In the optimized geometries of **5a–c** calculated by the PM7-COSMO method, the dihedral angle θ between pyrazine ring and the phenyl group at 8-position were 53.2°, 50.2°, and 46.1°, respectively, whereas those in the geometries obtained by DFT calculations were 29.1°, 30.0°, and 28.4°, respectively. Thus, DFT calculations gave more planar geometries than the PM7-COSMO method, and this does not correspond to the experimental results. The absorption spectra of **5a–c** were also calculated at different levels of theory and basis sets, which include a semi-empirical intermediate neglect of differential overlap/screened (INDO/S) approximation method [29], and the time-dependent DFT (TDDFT) method [23] at the B3LYP level with 6-31+G(d) basis set [27]. The above geometries, calculated by both the PM7-COSMO and the DFT methods, were used for these calculations. The results are summarized in Fig. 3 compiled with experimental data. Obviously, the INDO/S calculations using the geometries obtained by the PM7-COSMO provides absorption bands exhibiting good agreement with the experimental data. Thus, for the present system, the semi-empirical calculations are better approaches to obtain optimized geometries and absorption spectra than the DFT methods.

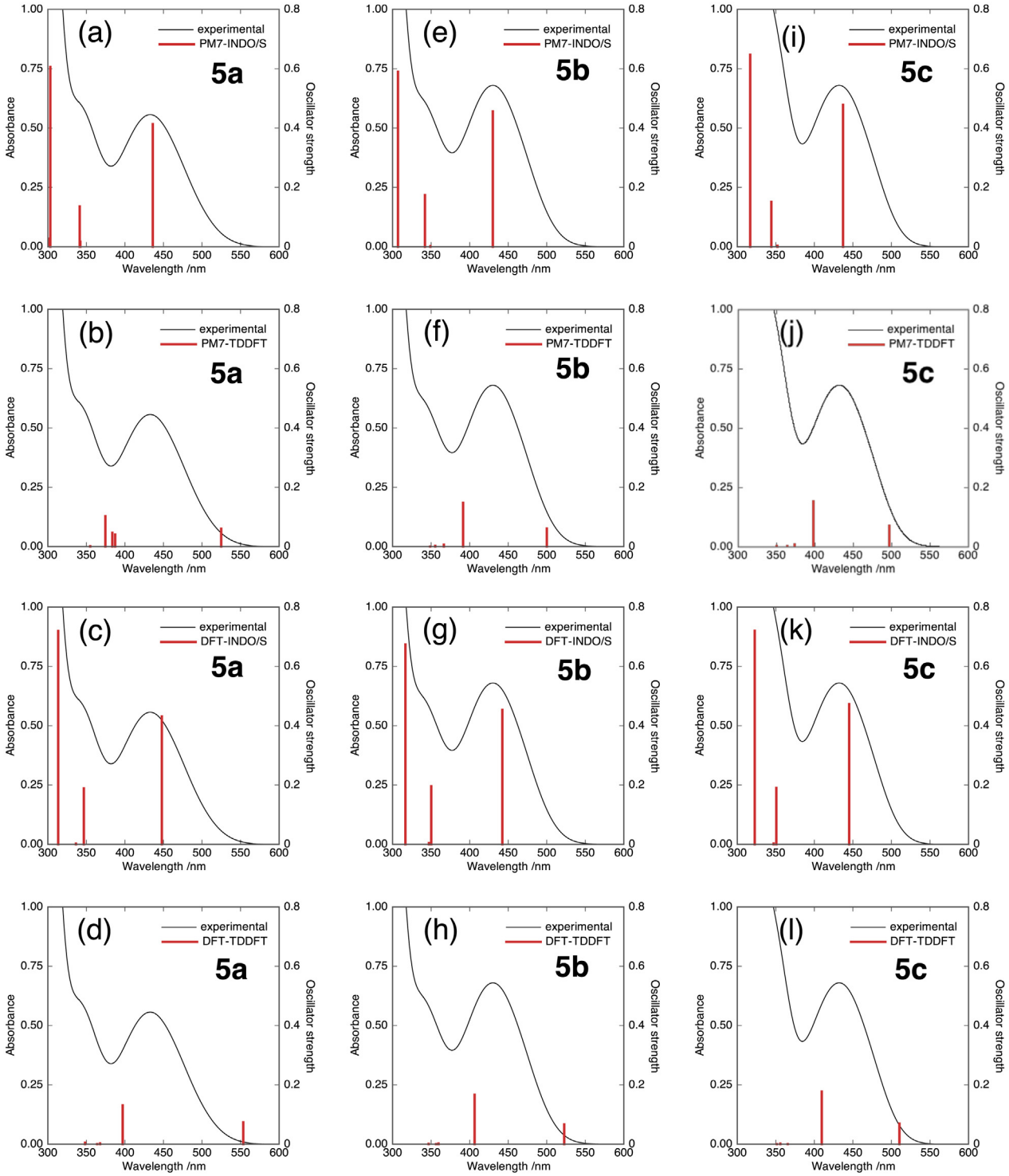

Fig. 3. Calculated absorption spectra (red sticks) of **5a–c** at different levels of theory: (a) **5a** (optimized by PM7-COSMO); INDO/S, (b) **5a** (PM7-COSMO); TD-B3LYP/6-31+G(d), (c) **5a** (B3LYP/6-31G(d)); INDO/S, (d) **5a** (B3LYP/6-31G(d)); TD-B3LYP/6-31+G(d), (e) **5b** (PM7-COSMO); INDO/S, (f) **5b** (PM7-COSMO); TD-B3LYP/6-31+G(d), (g) **5b** (B3LYP/6-31G(d)); INDO/S, (h) **5b** (B3LYP/6-31G(d)); TD-B3LYP/6-31+G(d), (i) **5c** (PM7-COSMO); INDO/S, (j) **5c** (PM7-COSMO); TD-B3LYP/6-31+G(d), (k) **5c** (B3LYP/6-31G(d)); INDO/S, (l) **5c** (B3LYP/6-31G(d)); TD-B3LYP/6-31+G(d). (For interpretation of the references to color in this figure legend, the reader is referred to the web version of this article.)

Table 1
Chemiluminescence properties of imidazopyrazinones **5a–c** and **3a–c** in aerated DMSO at 25 °C.

Compound (R)	CL_{max}[a] (nm)	Quantum yield			
		ϕ_{CL}[b]/10^{-2}	ϕ_R[c]	ϕ_{FL}[d]	ϕ_S[e]
5a (CF_3)	553	0.52	0.79	0.34	0.019
5b (H)	525	0.53	0.88	0.41	0.015
5c (OMe)	513	0.45	0.78	0.38	0.015
3a (CF_3)[f]	454	0.06	0.78	0.05	0.015
3b (H)[f]	462	0.15	0.93	0.18	0.008
3c (OMe)[f]	473	0.18	0.95	0.21	0.008

[a] Emission maxima of the chemiluminescence spectra.
[b] Chemiluminescence quantum yields.
[c] Chemical yields of the amidopyrazine products by chemiluminescent reactions.
[d] Fluorescence quantum yields of the corresponding light emitters.
[e] Quantum efficiency of chemical generation of the singlet-excited states of the light emitters.
[f] Values taken from Ref. [7].

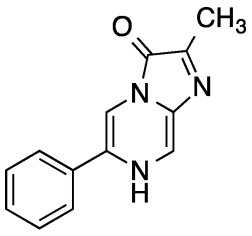

CLA

3.2. Substituent effect on chemiluminescence properties

3.2.1. Chemiluminescence maxima

The measurement of chemiluminescence of the synthesized imidazopyrazinones was achieved by mixing a methanolic stock solution of **5a–c** (1.0 mM) and DMSO under aerobic conditions [7]. The observed properties are summarized in Table 1. The chemiluminescence maxima (CL_{max}) of **5a–c** were observed at 553, 525, and 513 nm, respectively, as shown in Fig. 4. It has already been found that the introduction of a conjugating system at the 8-position of the imidazopyrazinone skeleton results in largely red-shifted chemiluminescence in DMSO [36]. As expected, the synthesized imidazopyrazinones produced light that was green, yellow, or yellowish green in DMSO, whereas 8-benzyl analogues **3** emitted blue light (λ_{max}: 454–479 nm) [7] under the same chemiluminescence reaction conditions. It is notable that a linear correlation was observed between the luminescence energy (in eV) for **5a–c** and Hammett's substituent constant (σ_p) of the substituent R (Fig. 5). This indicates that the color of

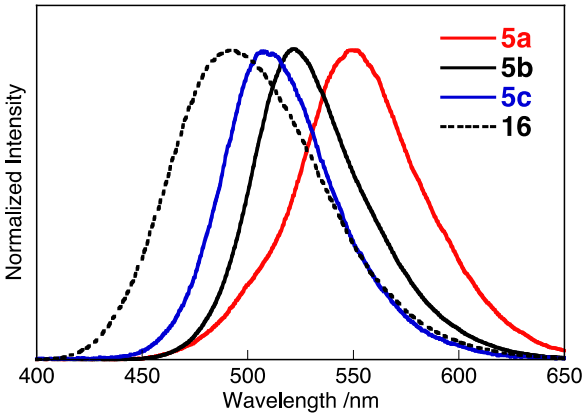

Fig. 4. Chemiluminescence spectra of **5a–c** and **16** in aerated DMSO at 25 °C.

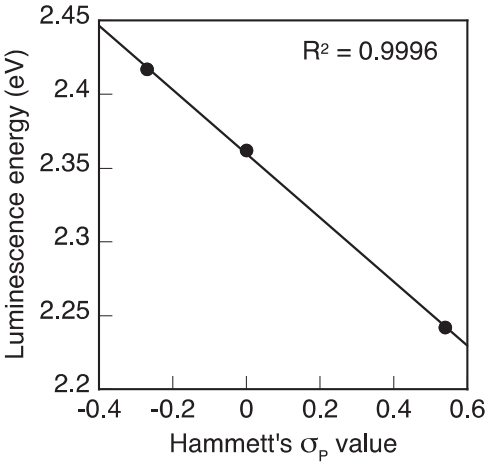

Fig. 5. Plots of the chemiluminescence energies (in eV) for **5a–c** measured in aerated DMSO against Hammett's substituent constant (σ_p values) of substituent R.

imidazopyrazinone chemiluminescence is freely controllable simply using the substituent effects.

These CL_{max} values corresponded well with the fluorescence maxima (FL_{max}) of the corresponding amide anion of **6a-c** measured in DMSO containing a methanolic solution of tetrabutylammonium hydroxide (Table 2), indicating that each imidazopyrazinone formed the singlet-excited state of the corresponding amide anion (**II**) in accordance with the proposed mechanism (Scheme 1). Therefore, the effect of the substituent on the CL_{max} corresponds to that on the FL_{max} of the amide anion. In order to better understand the effect of substituents on the electronic structures of the light emitters, amide anion forms of **6a–c**, the electronic absorption spectra of **6a–c** in DMSO containing methanolic tetrabutylammonium hydroxide as a base were measured. For comparison, the absorption spectra of coelenteramide analogues **4a–c**, which are the corresponding 3-benzyl derivatives, were also measured under the same condition. The results are compiled in Table 2, along with the fluorescence data and Stokes shift values.

As can be seen in Table 2, all the absorption maxima of **6a–c**$^-$ were observed at wavelengths that were shorter than the wavelengths at which those of the 3-benzyl derivatives **4a–c**$^-$ were observed. In addition, whereas the lowest transition energy was not affected strongly by the substituent, the fluorescence maxima were affected strongly. The electrostatic repulsion between the anion of the amide group and the phenyl group at the 3-position may have increased the transition energy and could be one of the causes of the hypsochromic absorption of **6**$^-$ as compared to **4**$^-$. This substituent-insensitive absorption clearly indicates that the observed transition does not have a charge transfer character, and therefore, the dipole change in **6**$^-$ with the substituent in the ground state is negligible. From these results, it can be inferred that the dihedral angle between the pyrazine ring and the phenyl group at the 3-position would be so large that they might not be able to effectively conjugate with each other. This consideration is supplementarily supported by a semi-empirical molecular orbital calculation. Fig. 6-a shows the optimized geometry of **6b**$^-$ in DMSO in the ground state (S_0) calculated by the PM7-COSMO method, in which the dihedral angle between the phenyl at the 3-position and the central pyrazine ring (θ) is 63.4°. On the other hand, the largely red-shifted CL_{max}, namely, the FL_{max} of **6**$^-$, strongly suggests that the phenyl group at the 3-position of the emitter conjugates effectively with the pyrazine ring. According to the PM7-COSMO calculation, the dihedral angle θ of **6b**$^-$ in the singlet-excited state (S_1) in DMSO is estimated to be 25.7°, as shown in Fig. 6-b, more

Table 2
Absorption and fluorescence data of **6a–c** and **4a–c** [16] in DMSO containing 0.5 vol% of 10%-methanolic tetrabutylammonium hydroxide at 25 °C.

Structure	Compound	R	Absorption maximum/nm (ε/10^{-4} cm^{-1} mol^{-1} l)	Fluorescence maximum (nm)	Stokes shift (10^3 cm^{-1})
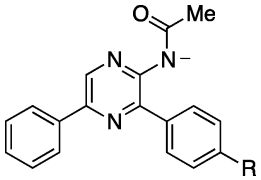	**6a**$^-$	CF_3	345 (2.00)	553	10.90
	6b$^-$	H	338 (1.77)	523	10.47
	6c$^-$	OMe	340 (1.74)	511	9.84
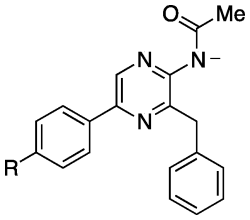	**4a**$^-$	CF_3	377 (1.91), 330 (sh. 1.59)	450[a]	4.30
	4b$^-$	H	364 (sh. 1.49), 314 (1.74)	462[a]	5.73
	4c$^-$	OMe	369 (sh. 1.48), 308 (2.02)	466[a]	5.64

[a] Values taken from Ref. [7].

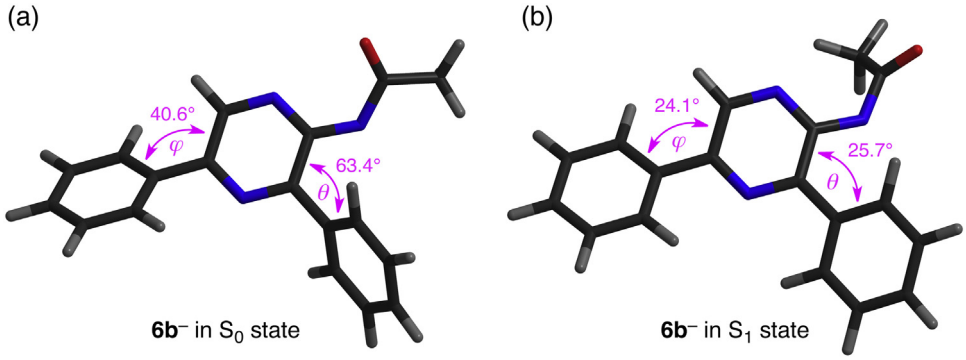

Fig. 6. Optimized geometry of the acetamidopyrazine anion **6b**$^-$ (a) in the ground state (S_0) and (b) in the singlet excited state (S_1), calculated by the PM7-COSMO method.

planar than that in the S_0 state. The dihedral angle φ between the 5-phenyl and pyrazine ring in the S_1 state was also calculated to be more planar (24.1°) than that in the S_0 state (40.6°), showing that the three aromatic rings in **6b**$^-$ overlap sufficiently in the S_1 state to extend the π-conjugation system. An attempt to get the optimized geometry of **6b**$^-$ in the S_1 by TDDFT method was also made. However, the calculation did not converge even after a week of CPU time.

Generally, a molecule in the excited state is more polar than that in the ground state [37,38]. 2-Acetamido-5-phenylpyrazines have dipole moments in the direction of the pyrazine ring from the phenyl group at the 5-position because of the electron-attracting ability of the pyrazine ring. Therefore, the repulsion between the dipole and the anion in the excited state should be greater than that in the ground state, and it is quite likely that **6**$^-$ adopts a more planar geometry in the lowest singlet-excited state in order to decrease the repulsion and to stabilize the anion by enabling charge delocalization through the extended conjugating system at the 3-position. Based on these considerations, the photophysical behavior of **6**$^-$ can be represented as shown in Fig. 7, where $S_{0,t}$ and $S_{0,p}$ denote the ground state of the twisted and the planar conformers, respectively, c is the velocity of light, and ν_{abs} and ν_{fl} are the wavenumbers corresponding to the absorption and emission maxima, respectively. After excitation, **6**$^-$ may get relaxed from the Franc–Condon state ($S_{1,FC}$) to the fully relaxed state ($S_{1,RX}$) accompanied by the twisting motion of the phenyl group especially at 3-position to extend the π-conjugation system affording the largely red-shifted fluorescence.

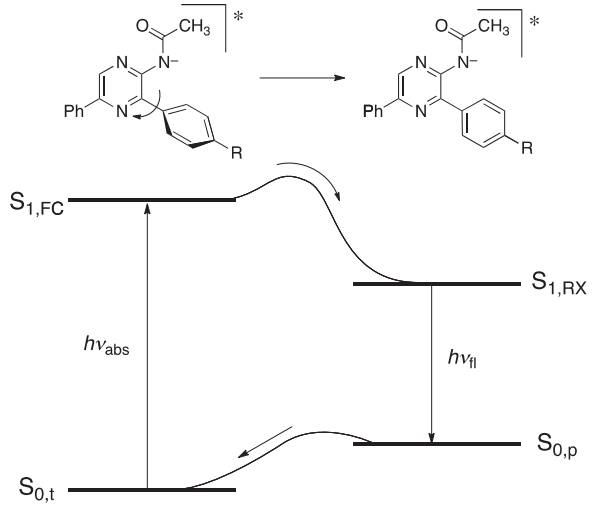

Fig. 7. Schematic explanation for the photophysical process of acetamidopyrazine **6**$^-$ in DMSO containing 0.5 vol% of 10%-methanolic tetrabutylammonium hydride.

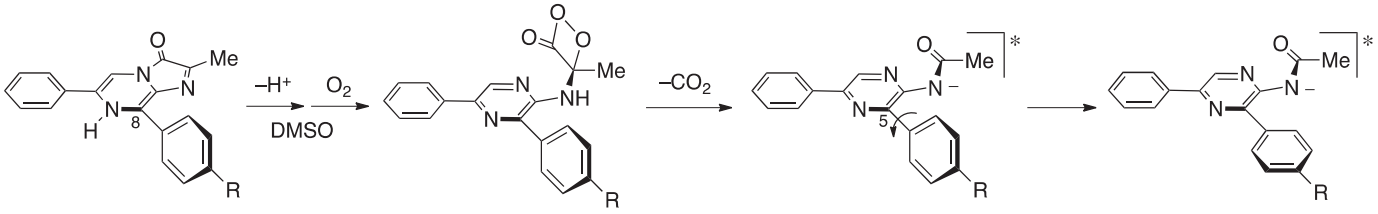

Fig. 8. Schematic illustration of a plausible reaction dynamics during the chemiluminescent reaction of **5**.

The same dynamics may be involved in the chemiluminescent reaction mechanism. At the initial stage of the chemiluminescent reaction, **5a–c** adopt twisted geometries at the 8-position. On proceeding with the reactions, singlet-excited amide anions are produced, which are likely to take up more planar conformations that are responsible for the largely red-shifted luminescence, as illustrated in Fig. 8.

To confirm this consideration, imidazopyrazinone **16**, which has two ortho-methyl groups on the 8-phenyl group to restrict the rotation of the 8-phenyl and take a twisted geometry at this position, was synthesized, as shown in Scheme 5, and its chemiluminescence was measured under the same conditions as those for **5a–c**. The obtained chemiluminescence spectrum was depicted in Fig. 4 together with those for **5a–c**. The CL_{max} for **16** was observed at 491 nm, which is still longer wavelength than that for **3b** but shorter than that for the corresponding analogue **5b**. This indicates that 2,6-dimethylphenyl moiety in the light emitter during the chemiluminescent reaction of **16** partly conjugates with the central pyrazine ring to shift its CL_{max} about 30 nm longer than that for **3b** but not to such an extent that cause the largely red-shifted one as **5b**. These facts led us to conclude that the chemiluminescent reaction mechanism of the present system involves the rotation of the substituted phenyl group at the 8-position (5-position for the amide anion).

Next, we discuss the effect of the substituent R on CL_{max}. As shown in Fig. 4, both CL_{max} and FL_{max} exhibited a strong dependence on the substituent R. Interestingly, the observed CL_{max} exhibited a bathochromic shift when R was changed from the electron-donating methoxy to the electron-withdrawing trifluoromethyl group, whereas the opposite substituent effect was observed in the case of the phenyl group at the 6-position of **3** wherein an electron-donating substituent R caused CL_{max} to exhibit a bathochromic shift [15]. As mentioned above, in the case of $\mathbf{6}^-$, shifts in CL_{max} result in corresponding shifts in FL_{max}, namely, the Stokes shifts. Generally, a Stokes shift in a fluorescence spectrum is essentially related to a change in the molecular dipole on excitation [38], which can be described well by the Lippert–Mataga equation [39]:

$$\nu_{abs} - \nu_{fl} = \frac{2}{hc}\frac{(\mu_e - \mu_g)^2}{a^3}\left(\frac{\varepsilon - 1}{2\varepsilon + 1} - \frac{n^2 - 1}{2n^2 + 1}\right) \quad (1)$$

where ν_{abs} and ν_{fl} are the wavenumbers corresponding to the absorption and emission maxima, respectively; μ_e–μ_g is the difference in dipole moment between the excited and the ground states; and ε, n, and a are the static bulk dielectric constant, optical refractive index of the solvent, and radius of the spherical cavity containing the dipole, respectively. Assuming the spherical radius a is constant, under the same conditions (i.e., in the same solvent and at the same temperature), the Stokes shift becomes a function of μ_g and μ_e. In the present system, the changes in the ground state dipoles among **6a–c**$^-$ as a result of the substituents are small, as can be seen from the substituent-insensitive absorption behavior (Table 2), and therefore, the large, substituent-sensitive Stokes shifts observed are considered to be caused predominantly by the molecular dipole changes in the excited states according to Eq. (1). That is, the difference in the peak shift among **6a–c**$^-$ reflects the difference in the dipole moments in the excited states. In general, the reorganization of the solvent molecules around a solute proceeds upon excitation according to the newly formed dipole vector and thereby stabilize the solute in the singlet-excited state [38]. The degree of this stabilization depends on the magnitude of the newly formed dipole moment. In general, the greater the polarity of a molecule in the singlet-excited state, the greater the stabilization of the excited state energy in a polar solvent such as DMSO. This results in the large Stokes shift [38]. In the case of 2-acetamido-5-phenylpyrazines, the dipole moments are directed toward the pyrazine ring from the phenyl group at the 5-position. In the case of **4**, an electron-donating substituent on the phenyl group at the 5-position increases the molecular dipole moment of the light emitter in the singlet-excited state [16], causing red-shifted chemiluminescence. In the present system, the larger Stokes shift observed for the trifluoromethyl analog (**6a**$^-$) as compared to that observed for the methoxy analog (**6c**$^-$) apparently indicates that the former has a larger dipole moment than the latter in the singlet-excited state. Fig. 9 displays this dipole change schematically. Assuming, for the sake of convenience, a coordinate axis defined as shown in Fig. 9-a, an electron-withdrawing substituent *Y* on the phenyl group at the 3-position synergistically increases the magnitude of the x-axis component of the molecular dipole moment (Fig. 9-b). Thus, it is evident that CL_{max} (i.e., FL_{max} of the corresponding amide anions) of imidazo[1,2-*a*]pyrazin-3(7*H*)-ones shifts to a longer wavelength with an increase in the dipole moments of the corresponding

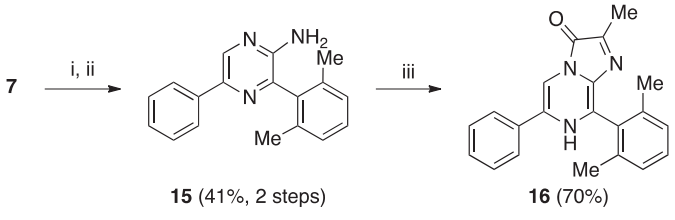

Scheme 5. Synthesis of imidazopyrazinone **16**. *Reagents and conditions*: (i) 2,6-dimethylphenylboronic acid (1 eq.), $PdCl_2(PPh_3)_2$, PPh_3, Na_2CO_3, aqueous dioxane, reflux, 16 h; (ii) phenylboronic acid (1 eq.), $Pd(PPh_3)_4$, Na_2CO_3, aqueous dioxane, reflux, 19 h; (iii) pyruvic aldehyde, HCl, EtOH, 90 °C, 4 h.

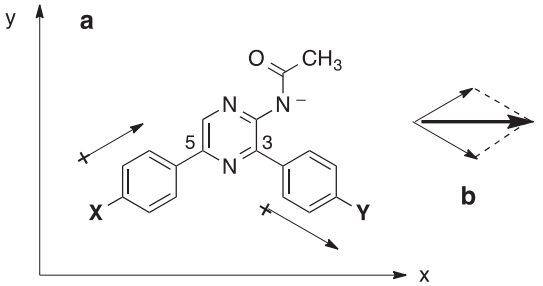

Fig. 9. Schematic explanation of dipole interactions in the acetamidopyrazine anion, **6**$^-$.

emitter in the singlet-excited states as a result of the substituents, and the seemingly opposite substituent effect on the CL_{max} observed in **3** and **5** is now explained.

3.2.2. Chemiluminescence quantum yields

The chemiluminescence quantum yield (ϕ_{CL}) is generally defined as the product of three efficiencies, i.e., the fraction of reacting molecules that follow the correct chemical pathway (ϕ_R), quantum yield of the singlet-excited molecule formed (ϕ_S), and fluorescence quantum yield of the light emitter (ϕ_{FL}) [37]:

$$\phi_{CL} = \phi_R \phi_S \phi_{FL} \quad (2)$$

The values of ϕ_{CL}, ϕ_R, and ϕ_{FL} for the present system were experimentally obtained (see Section 2), and the ϕ_S values were calculated using these data and Eq. (2). The results are compiled in Table 1, accompanied by those for the 8-benzyl analogues **3a–c** obtained under the same conditions [7]. All compounds underwent the chemiluminescent reaction with good ϕ_R values. It should be emphasized that the ϕ_{CL} values of **5a–c** were 3–8 times larger than those of **3a–c**, and thus, the 8-arylated compounds **5a–c** are found to be highly effective chemiluminescent substrates relative to the 8-alkyl derivatives **3a–c**. With respect to the ϕ_{FL} values of **5a–c**, they are obviously larger than those of **3a–c**. This result clearly indicates that the observed enhancement in the ϕ_{CL} values for **5a–c** reflects the improved ϕ_{FL} values of the light emitters.

The ϕ_S values observed for **5**, which are the focus of our attention, proved to be almost equal to those observed for **3**. In addition, only a small change with substituents was observed. In order to understand this substituent-insensitive ϕ_S, the electronic properties of the corresponding dioxetane intermediates **17a–c** during the chemiluminescent reaction of **5a–c** were calculated by the DFT method at the B3LYP level with a 6-31+G(d) basis set. For comparison, the same calculations for **18a–c**, the model structures of dioxetane intermediates during the chemiluminescent reaction of **3**, were conducted. The calculated total Mulliken charge densities of the amide nitrogen (q_N) and the atoms that constitute the dioxetanone moiety (q_{Dox}) are summarized in Table 3. The q_N values of **17** as well as **18** also scarcely varied with substituent changing from electron-withdrawing trifluoromethyl (Hammett substituent constant $\sigma_p = 0.54$) [40] to electron-donating methoxy ($\sigma_p = -0.27$) [40] groups. The q_{Dox} values also exhibited a slight change with substituents. Thus, it is conjectured that the small charge changes on the amide nitrogen and on the dioxetane moiety with substituents are in accordance with the small substituent effect on ϕ_S.

Teranishi and Goto have reported similar weak substituent effects on the ϕ_S values for the chemiluminescence of 5-(5-aryl-2-pyrazinylamino)-1,2,4-trioxane derivatives **19**, which chemiluminesced in the presence of a base via the dioxetane intermediate **20**. The observed ϕ_S values varied from 0.0026 to 0.0067 [41]. They attributed these observations to the fact that the negative charge on the nitrogen atom gives it an electron-donating ability that is sufficiently strong to readily decompose the dioxetane by itself without the need for any support from electron-donating substituents. This consideration is applicable to our system.

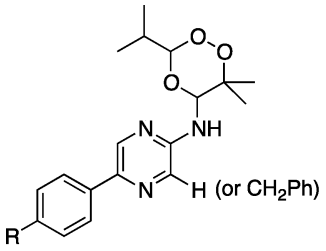

19 (R = Br, H, OMe, OH, NMe_2)

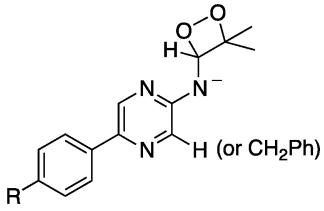

20

Thus, our observations do not validate the conventional explanation that an electron-donating substituent on a phenyl group bound to the central pyrazine ring enhances the ϕ_S. However, this does not deny the applicability of the CIEEL or CTIL mechanism because the nitrogen anion serves as a strong electron donor. In this regard, many studies have focused on the chemiluminescence of dioxetanes, whose ϕ_S values exhibited a strong dependency on the electronic character of the substituents. For instance, 1,2-dioxetane **21**, which has two *p*-substituted phenyl groups directly linked to the central dioxetane ring, exhibited a drastic enhancement in its ϕ_S value when R was a strongly electron-donating dimethylamino group [42]. Thus, the CIEEL or CTIL mechanism can still be applicable for explaining the effective decomposition of dioxetanes to generate singlet-excited light emitters but not for the high ϕ_S value in the aequorin bioluminescence. Previously, Matsumoto et al. demonstrated that in the case of the chemiluminescence of 1,1-linked dioxetane derivatives **22**, it is essential to determine the conformation of the electron-donating phenolate anion moiety relative to the dioxetane ring in order to determine the luminescence efficiency [43]. Yamaguchi et al. also demonstrated that efficiently luminescent dioxetanes take appropriate conformations for efficient singlet-excited energy productions during their thermal decomposition reactions [11]. Taking these facts and our present results into consideration, a possible explanation for the high ϕ_S value in the aequorin bioluminescence is that the conformation of the dioxetanone intermediate is strictly regulated by the surrounding apoprotein, apoaequorin, in such a manner that it is favorable

Table 3
DFT calculations of the electronic properties of the dioxetane intermediate **17** and **18** having substituent R (CF_3, H, or OMe) at the B3LYP/6-31+G(d) level.

Structure	Compound	R	q_N	q_{Dox}
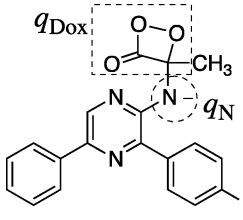	**17a**	CF_3	−0.352	−0.138
	17b	H	−0.362	−0.135
	17c	OMe	−0.356	−0.142
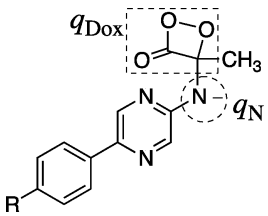	**18a**	CF_3	−0.352	−0.255
	18b	H	−0.368	−0.267
	18c	OMe	−0.368	−0.272

for generating the singlet-excited light emitter, whereas in the absence of the protein, the corresponding dioxetane intermediate may take up an arbitrary conformation that predominantly afford the light emitter not in the singlet-excited state but in the ground state.

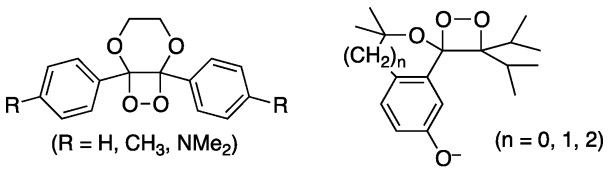

21 **22**

4. Conclusions

We have presented the syntheses and the chemiluminescence properties of **5a**–**c**. The chemiluminescence efficiencies (ϕ_{CL}) of these imidazopyrazinones were definitely improved by the introduction of a *p*-substituted phenyl group at the 8-position, but this improvement was not caused a change in the value of ϕ_S but by that in the value of ϕ_{FL}. In contrast to the substituent-sensitive ϕ_{FL}, ϕ_S exhibited weak substituent dependency, and those absolute values remained small. Therefore, it seems reasonable to conclude that it is impossible to construct efficient imidazopyrazinone-chemiluminescence systems comparable to aequorin-bioluminescence systems only by changing the electronic character of substituents. Although the regulation of ϕ_S by changing the electronic property of substituents was not achieved, it was proved that the chemiluminescence maximum, CL_{max}, was controllable using the substituent effect. In proportion to the electron-attracting ability of the substituent at the *para*-position of the 8-phenyl group, CL_{max} was shifted to longer wavelength. Interestingly, the direction of this spectral shift with the electronic property of the substituent is opposite to that observed for coelenterazine analogues **3** whose CL_{max} was shifted to longer wavelength with increasing the electron-donating ability of the substituent at the *para*-position of the 6-phenyl group. These findings provide a new principle as a guide for designing imidazopyrazinones capable of emitting further red-shifted chemiluminescence required in the field of analytical chemistry.

Acknowledgements

The authors gratefully acknowledge support for this research by a Grant-in-Aid for Scientific Research C (No 25410179 for R.S. and No. 22550031 for T.H.) from the Japan Society for the Promotion of Science (JSPS). Financial support to R.S. from MEXT-Supported Program for the Strategic Research Foundation at Private Universities (2012–2016) is also gratefully appreciated. We would like to thank Mr. Grant White for his kind assistance in correcting this manuscript.

References

[1] Y. Ohmiya, T. Hirano, Shining the light: the mechanism of the bioluminescence reaction of calcium-binding photoproteins, Chem. Biol. 3 (1996) 337–347.
[2] O. Shimomura, F.H. Johnson, Calcium binding, quantum yield, and emitting molecule in aequorin bioluminescence, Nature 227 (1970) 1356–1357.
[3] O. Shimomura, F.H. Johnson, Chemical nature of light emitter in bioluminescence of aequorin, Tetrahedron Lett. (1973) 2963–2966.
[4] K. Teranishi, T. Goto, Effects of conformational rigidity and hydrogen-bonding in the emitter on the chemi-luminescence efficiency of coelenterazine (*Oplophorus* luciferin), Chem. Lett. (1989) 1423–1426.
[5] (a) F. McCapra, Y.C. Chang, The chemiluminescence of a *Cypridina* luciferin analogue, Chem. Commun. (1967) 1011–1012;
(b) T. Goto, Y. Kishi, Luciferins, bioluminescent substances, Angew. Chem. Int. Ed. Engl. 7 (1968) 407–414.
[6] K. Usami, M. Isobe, Low-temperature photooxygenation of coelenterate luciferin analog synthesis and proof of 1,2-dioxetanone as luminescence intermediate, Tetrahedron 52 (1996) 12061–12090.
[7] R. Saito, T. Hirano, S. Maki, H. Niwa, M. Ohashi, influence of electron-donating and electron-withdrawing substituents on the chemiluminescence behavior of coelenterazine analogs, Bull. Chem. Soc. Jpn. 84 (2011) 90–99.
[8] Y. Ishii, C. Hayashi, Y. Suzuki, T. Hirano, Chemiluminescent 2,6-diphenylimidazo[1,2-*a*]pyrazin-3(7*H*)-ones: a new entry to *Cypridina* luciferin analogues, Photochem. Photobiol. Sci. 13 (2014) 182–189.
[9] (a) J.Y. Koo, G.B. Schuster, Chemiluminescence of diphenoyl peroxide. Chemically-initiated electron exchange luminescence. New general mechanism for chemical production of electronically excited-states, J. Am. Chem. Soc. 100 (1978) 4496–4503;
(b) G.B. Schuster, Chemi-luminescence of organic peroxides. Conversion of ground-state reactants to excited-state products by the chemically-initiated electron-exchange luminescence mechanism, Acc. Chem. Res. 12 (1979) 366–373.
[10] (a) L.H. Catalani, T. Wilson, Electron-transfer and chemi-luminescence. Two inefficient systems: 1,4-dimethoxy-9,10-diphenylanthracene peroxide and diphenoyl peroxide, J. Am. Chem. Soc. 111 (1989) 2633–2639;
(b) Y. Takano, T. Tsunesada, H. Isobe, Y. Yoshioka, K. Yamaguchi, I. Saito, Theoretical studies of decomposition reactions of dioxetane, dioxetanone, and related species. CT induced luminescence mechanism revisited, Bull. Chem. Soc. Jpn. 72 (1999) 213–225;
(c) T. Hirano, Y. Takahashi, H. Kondo, S. Maki, S. Kojima, H. Ikeda, H. Niwa, The reaction mechanism for the high quantum yield of *Cypridina* (*Vargula*) bioluminescence supported by the chemiluminescence of 6-aryl-2-methylimidazo[1,2-a]pyrazin-3(7*H*)-ones (Cypridina luciferin analogues), Photochem. Photobiol. Sci. 7 (2008) 197–207.
[11] H. Isobe, Y. Takano, M. Okumura, S. Kuramitsu, K. Yamaguchi, Mechanistic insights in charge-transfer-induced luminescence of 1,2-dioxetanones with a substituent of low oxidation potential, J. Am. Chem. Soc. 127 (2005) 8667–8679.
[12] G.B. Schuster, B. Dixon, J.Y. Koo, S.P. Schmidt, J.P. Smith, Chemical mechanisms of chemi-luminescence and bioluminescence. Reactions of high-energy content organic-compounds, Photochem. Photobiol. 30 (1979) 17–26.
[13] (a) T. Hirano, I. Mizoguchi, M. Yamaguchi, F.Q. Chen, M. Ohashi, Y. Ohmiya, F.I. Tsuji, Revision of the structure of the light-emitter in aequorin bioluminescence, J. Chem. Soc., Chem. Commun. (1994) 165–167;
(b) K. Mori, S. Maki, H. Niwa, H. Ikeda, T. Hirano, Real light emitter in the bioluminescence of the calcium-activated photoproteins aequorin and obelin: light emission from the singlet-excited state of coelenteramide phenolate anion in a contact ion pair, Tetrahedron 62 (2006) 6272–6288.
[14] F. McCapra, Alternative mechanism for dioxetan decomposition, J. Chem. Soc., Chem. Commun. (1977) 946–948.
[15] R. Saito, T. Hirano, H. Niwa, M. Ohashi, Substituent effects on the chemiluminescent properties of coelenterazine analogs, Chem. Lett. (1998) 95–96.
[16] R. Saito, T. Hirano, H. Niwa, M. Ohashi, Solvent and substituent effects on the fluorescent properties of coelenteramide analogs, J. Chem. Soc., Perkin Trans. 2 (1997) 1711–1716.
[17] R. Saito, C. Inoue, A. Katoh, Well-divided and pH-dependent bimodal chemiluminescence of 2-methyl-6-phenyl-8-(4-substituted phenyl)imidazo[1,2-a]pyrazin-3(7*H*)-ones induced by superoxide anion, Heterocycles 63 (2004) 759–764.
[18] R. Saito, N. Suga, A. Katoh, S. Maki, T. Hirano, H. Niwa, 6,8-Diarylimidazo[1,2-a]pyrazin-3(7*H*)-ones as potential chemiluminescent ph/superoxide double sensors, in: A. Tsuji, M. Matsumono, M. Maeda, L.J. Kricka, P.E. Stanley (Eds.), Proceedings of the 13th International Symposium on Bioluminescence & Chemiluminescence. Progress and Perspectives, World Scientific, Singapore, 2005, pp. 335–338.
[19] J.J.P. Stewart, Optimization of parameters for semiempirical methods VI: more modifications to the NDDO approximations and re-optimization of parameters, J. Mol. Model. 19 (2013) 1–32.
[20] J.J.P. Stewart, MOPAC 2012, in: Stewart Computational Chemistry, Colorado Springs, CO, USA, 2012.
[21] A. Klamt, G. Schuurmann, COSMO. A new approach to dielectric screening in solvents with explicit expressions for the screening energy and its gradient, J. Chem. Soc., Perkin Trans. 2 (1993) 799–805.
[22] F. Jensen, Introduction to Computational Chemistry, second ed., John Wiley and Sons, Ltd., Wast Sussex, UK, 2007.
[23] P. Elliott, F. Furche, K. Burke, Excited states from time-dependent density functional theory, in: K.B. Lipkowitz, T.R. Cundari (Eds.), Reviews in Computational Chemistry, Jon Wiley and Sons, Hoboken, NJ, 2009.
[24] M.W. Schmidt, K.K. Baldridge, J.A. Boatz, S.T. Elbert, M.S. Gordon, J.H. Jensen, S. Koseki, N. Matsunaga, K.A. Nguyen, S.J. Su, T.L. Windus, M. Dupuis, J.A. Montgomery, General atomic and molecular electronic-structure system, J. Comput. Chem. 14 (1993) 1347–1363.
[25] (a) M.S. Gordon, M.W. Schmidt, Advances in electronic structure theory: GAMESS a decade later, in: C.E. Dykstra, G. Frenking, K.S. Kim, G.E. Scuseria (Eds.), Theory and Applications of Computational Chemistry, Elsevier, Amsterdam, 2005, pp. 1167–1189;
(b) M.E. Lasinski, N.A. Romero, S.T. Brown, J.P. Blaudeau, Recent performance improvements to the DFT and TDDFT in GAMESS, J. Comput. Chem. 33 (2012) 723–731.
[26] (a) C.T. Lee, W.T. Yang, R.G. Parr, Development of the colle-salvetti correlation-energy formula into a functional of the electron-density, Phys. Rev. B: Condens. Matter 37 (1988) 785–789;

(b) A.D. Becke, Density-functional thermochemistry. 3. The role of exact exchange, J. Chem. Phys. 98 (1993) 5648–5652;
(c) P.J. Stephens, F.J. Devlin, C.F. Chabalowski, M.J. Frisch, *Ab-initio* calculation of vibrational absorption and circular-dichroism spectra using density-functional force-fields, J. Phys. Chem. 98 (1994) 11623–11627;
(d) R. Hertwig, W. Koch, On the parameterization of the local correlation functional. What is Becke-3-LYP? Chem. Phys. Lett. 268 (1997) 345–351.
[27] R.D. Adamson, P.M.W. Gill, J.A. Pople, Empirical density functionals, Chem. Phys. Lett. 284 (1998) 6–11.
[28] N. Senda, Winmostar version 4.100, in, X-Ability Co. Ltd., Tokyo, Japan, 2013.
[29] (a) J. Ridley, M. Zerner, Intermediate neglect of differential overlap technique for spectroscopy. Pyrrole and azines, Theor. Chim. Acta 32 (1973) 111–134;
(b) A.D. Bacon, M.C. Zerner, intermediate neglect of differential overlap theory for transition-metal complexes. Fe, Co and Cu chlorides, Theor. Chim. Acta 53 (1979) 21–54;
(c) M.C. Zerner, G.H. Loew, R.F. Kirchner, U.T. Muellerwesterhoff, Intermediate neglect of differential-overlap technique for spectroscopy of transition-metal complexes. Ferrocene, J. Am. Chem. Soc. 102 (1980) 589–599.
[30] (a) J. Lee, H.H. Seliger, Absolute spectral sensitivity of phototubes and the application to the measurement of the absolute quantum yields of chemiluminescence and bioluminescence, Photochem. Photobiol. 4 (1965) 1015–1048;
(b) J. Lee, H.H. Seliger, Quantum yields of the luminol chemiluminescence reaction in aqueous and aprotic solvents, Photochem. Photobiol. 15 (1972) 227–237.
[31] J.F. Cavalier, M. Burton, C. De Tollenaere, F. Dussart, C. Marchand, J.F. Rees, J. Marchand-Brynaert, 2,6-Diamino-3,5-diaryl-1,4-pyrazine derivatives as novel antioxidants, Synthesis (2001) 768–772.
[32] J. Berthelot, C. Guette, P.L. Desbene, J.J. Basselier, P. Chaquin, D. Masure, Regioselective bromination in aromatic series. 1. *para*-Monobromination of phenols and aromatic-amines using tetrabutylammonium tribromide, Can. J. Chem. 67 (1989) 2061–2066.
[33] (a) N. Sato, Studies on pyrazines. 8. An improved syntheses of 2-amino-3,5-dibromo-pyrazine and 2-amino-5-bromopyrazine, J. Heterocycl. Chem. 19 (1982) 673–674;
(b) H. Nakamura, D. Takeuchi, A. Murai, Synthesis of 5-substituted and 3,5-substituted 2-aminopyrazines by Pd mediated Stille coupling, Synlett (1995) 1227–1228.
[34] H. Nakamura, M. Aizawa, D. Takeuchi, A. Murai, O. Shimoura, Convergent and short-step syntheses of DL-Cypridina luciferin and its analogues based on Pd-mediated cross couplings, Tetrahedron Lett. 41 (2000) 2185–2188.
[35] K. Akutsu, H. Nakajima, T. Katoh, S. Kino, K. Fujimori, Chemiluminescence of *Cypridina* luciferin analogs. 2. Kinetic-studies on the reaction of 2-methyl-6-phenylimidazo[1,2-*a*]pyrazin-3(7*H*)-one (CLA) with superoxide—hydroperoxyl radical is an actual active species used to initiate the reaction, J. Chem. Soc., Perkin Trans. 2 (1995) 1699–1706.
[36] H. Nakamura, C. Wu, D. Takeuchi, A. Murai, Bimodal chemiluminescence of 8-chlorostyryl-6-phenylethynylimidazopyrazinone: large bathochromic shift caused by a styryl group at 8-position, Tetrahedron Lett. 39 (1998) 301–304.
[37] N.J. Turro, Modern Molecular Photochemistry, University Science Books, Sausalito, CA, 1991.
[38] J.R. Lakowicz, Principles of Fluorescence Spectroscopy, third ed., Springer, New York, NY, 2006.
[39] (a) E. Lippert, Dipolmoment und elektronenstruktur von angeregten molekülen, Z. Naturforsch. 10a (1955) 541–545;
(b) E. Lippert, Spektroskopische bestimmung des dipolmomentes aromatischer verbindungen im ersten angeregten singulettzustand, Z. Elektrochem. 61 (1957) 962–975;
(c) N. Mataga, Y. Kaifu, M. Koizumi, The solvent effect on fluorescence spectrum. Change of solute-solvent interaction during the lifetime of excited solute molecule, Bull. Chem. Soc. Jpn. 28 (1955) 690–691;
(d) N. Mataga, Y. Kaifu, M. Koizumi, Solvent effects upon fluorescence spectra and the dipolemoments of excited molecules, Bull. Chem. Soc. Jpn. 29 (1956) 465–470.
[40] J.E. Leffler, E. Grunwald, Rates and Equilibria of Organic Reactions: As Treated by Statistical, Thermodynamic and Extrathermodynamic Methods, John Wiley and Sons, Inc., New York, NY, 1963.
[41] K. Teranishi, T. Goto, No electron-donating substituent effect on the singlet excited-state formation from the 5-(5-aryl-2-pyrazinylamino)-1,2,4-trioxanes in dimethylsulfoxide triggered by potassium *tert*-butoxide, Bull. Chem. Soc. Jpn. 62 (1989) 2009–2012.
[42] (a) K.A. Zaklika, A.L. Thayer, A.P. Schaap, Substituent effects on decomposition of 1,2-dioxetanes, J. Am. Chem. Soc. 100 (1978) 4916–4918;
(b) K.A. Zaklika, T. Kissel, A.L. Thayer, P.A. Burns, A.P. Schaap, Mechanisms of 1,2-dioxetane decomposition. Role of electron transfer, Photochem. Photobiol. 30 (1979) 35–44.
[43] M. Matsumoto, N. Watanabe, T. Shiono, H. Suganuma, J. Matsubara, Chemiluminescence of spiro[1,2-dioxetane-3,1′-dihydroisobenzofuran]s, spiro[1,2-dioxetane-3,1′-isochroman]s and a spiro[1,2-dioxetane-3,1′-(2-benzoxepane)], Tetrahedron Lett. 38 (1997) 5825–5828.